Journal of Solid and Fluid Mechanics (JSFM), 15(4): 23-26, 2025

Shahrood University of Technology

Journal of Solid and Fluid Mechanics (JSFM)

DOI: 10.22044/jsfm.2025.15640.3935

Manufacturing Engineering of Iran

Numerical investigation of the effect of opposing gas flow directions in adjacent cells on power generation and temperature distribution in a polymer electrolyte membrane fuel cell

Mohammad Amin Zibaei[1], Javad Mahmoudimehr[2], Masoud Hami[3]

[1]MSc graduate, Faculty of Mechanical Engineering, Guilan University, Rasht, Iran
[2]Assoc. Prof., Faculty of Mechanical Engineering, Guilan University, Rasht, Iran
[3]Ph.D graduate, Faculty of Mechanical Engineering, Guilan University, Rasht, Iran

*Corresponding author: mahmoudimehr@guilan.ac.ir

Received: 01/21/2025 Revised: 07/07/2025 Accepted: 08/31/2025

Abstract

This study numerically investigates the effect of different inlet gas flow directions on the thermal and electrochemical behavior of two adjacent polymer electrolyte membrane fuel cells (PEMFCs). The governing equations are solved under steady-state, three-dimensional conditions using the finite volume method in ANSYS Fluent. The results reveal a distinct trade-off between thermal uniformity and electrochemical performance, where an improvement in one aspect is accompanied by a decline in the other. A comparative analysis of five inlet flow configurations shows that the most uniform temperature distribution, corresponding to the lowest thermal gradient, occurs when the flow directions in both cells and rows are aligned (Case 1). In this case, the maximum difference in temperature gradient relative to other configurations is 4.4 K/cm. Conversely, the highest current density is achieved when the flow directions in both cells and rows are opposite (Case 5), with a maximum difference of 0.29 A/cm² (30.21%) at an operating voltage of 0.75 V. These findings provide valuable guidance for designing flow configurations that balance thermal management and electrochemical performance in PEMFCs.

Keywords: Adjacent cells; Current density; Numerical investigation; Polymer electrolyte membrane fuel cell (PEMFC); Temperature gradient

1. Introduction

The rapid growth of population and industrial activities has led to a substantial increase in global energy demand, which is still largely dependent on fossil fuels. However, the non-renewable nature of these resources, together with their limited efficiency and considerable greenhouse gas emissions, highlights the urgent need for cleaner and more efficient energy conversion technologies [1,2].

Fuel cells, as electrochemical devices that directly convert chemical energy into electricity, offer several advantages including high efficiency, low emissions, silent operation, and long-term durability [3,4]. Among them, proton exchange membrane fuel cells (PEMFCs) have gained significant attention due to their high power density, low operating temperature, and rapid start-up capability, making them a promising candidate for sustainable energy systems [5–7].

Nevertheless, the operation of PEMFCs at high current densities is often associated with non-uniform temperature distributions and steep temperature gradients, which can negatively impact their performance and reduce lifespan. Therefore, achieving a balance between current density and temperature uniformity is crucial to ensure stable and reliable operation [8].

In this context, direction of inlet flows play a critical role, as they influence reactant distribution and temperature homogeneity. Appropriate flow direction can mitigate localized heating, thereby improving both durability and performance [9].

In recent years, several experimental and numerical studies have been dedicated to enhancing PEMFC performance through modifications to flow-field geometry and flow management. Bilgili et al. [10] demonstrated that incorporating obstacles into flow channels improves gas concentration distribution and reactant transport to active regions, leading to higher current density. Rezazadeh et al. [11] investigated the influence of gas channel geometry on PEMFC performance through both numerical simulations and experimental tests. They observed that sinusoidal walls increase the reactant pathway, which in turn enhances diffusion to the catalyst layers and ultimately improves overall cell performance. Pashaki and Mahmoudimehr [12] numerically compared curved and straight PEMFC configurations and found that bending with a 20° angle resulted in an 8.33% improvement in performance. Fu et al. [13] showed that parallel sinusoidal wavy channels enhance mass transfer relative to straight

channels, yielding a 6.16% increase in net power density. Yang et al. [14] reported that a chain-shape flow field configuration facilitates superior oxygen transport and current density distribution compared to a parallel design, resulting in an 18.9% increase in power density.

Based on the literature review, previous studies have primarily focused on the electrochemical performance of PEMFCs, while their thermal behavior has received comparatively little attention. However, increasing the current density can cause excessive temperature gradients within the cell structure. Furthermore, to the best of the authors' knowledge, the impact of opposite inlet flow directions in adjacent cells has not yet been explored. To address this research gap, the present study conducts a three-dimensional numerical simulation of two PEMFCs to investigate the influence of inlet flow direction on both thermal and electrochemical performance. The analysis seeks to identify the optimal flow configuration with respect to current density distribution and temperature gradients.

2. Problem definition

Figure 1(a) presents a three-dimensional schematic of two adjacent PEMFCs. Each cell is composed of a membrane, an anode electrode, a cathode electrode, and corresponding anode and cathode flow channels. The electrodes consist of a gas diffusion layer and a catalyst layer [15]. In this configuration, the anode channels are arranged in the upper row, while the cathode channels are located in the lower row.

Based on the direction of the reactant gas entering the flow channels, five distinct flow configurations can be defined. Figure 1(b) illustrates a three-dimensional representation of these five possible inlet flow orientations for the adjacent cells.

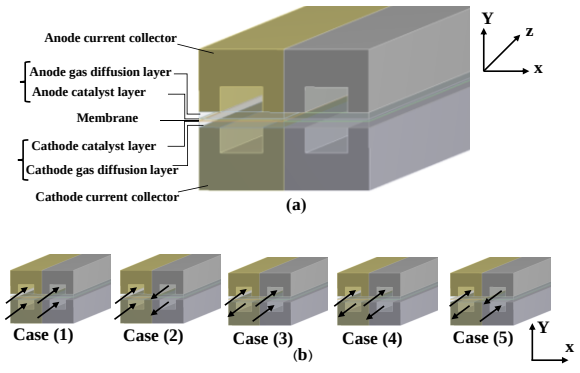

Figure 1. (a) Schematic of PEMFC components and (b) different inlet flow configurations for two adjacent cells

3. Simulation

In this section, the governing equations, and solution methodology are examined. The mass conservation equation is presented in Equation (1), where $\vec{u}$ denotes the velocity vector and ρ represents the mixture density, calculated using Equation (2). Furthermore, $S_{H_2O}, S_{O_2}, S_{H_2O}$ are the source terms corresponding to hydrogen consumption, oxygen consumption, and water production, respectively, which are determined from Equations (3) to (5) [16, 17].

$$\vec{\nabla} \cdot (\rho \vec{u}) = S_{H_2} + S_{0_2} + S_{H_2O} \quad (1)$$

$$\rho = \frac{P}{RT \sum \frac{Y_i}{M_i}} \quad (2)$$

$$S_{H_2} = -\frac{j_{an}}{2F} M_{H_2} \quad (3)$$

$$S_{O_2} = -\frac{j_{ca}}{4F} M_{O_2} \quad (4)$$

$$S_{H_2O} = +\frac{j_{ca}}{2F} M_{H_2O} \quad (5)$$

The momentum equation is expressed in Equation (6), where S_u is momentum source term [12]:

$$\vec{\nabla} \cdot (\rho \vec{u}\vec{u}) = -\vec{\nabla} P + \vec{\nabla} \cdot (\vec{\nabla} \mu \vec{u}) + S_u \quad (6)$$

$$S_u = -\frac{\mu}{k_p} \varepsilon \vec{u} \quad (7)$$

Equation (8) represents the species transport equation. In this equation, D_i denotes the diffusivity of species, and D_i^{eff} is the effective diffusivity, which is obtained from Equation (9) [12,18]:

$$\vec{\nabla} \cdot (\rho \vec{u} Y_i) = \vec{\nabla} \cdot (\rho D_i^{eff} \nabla Y_i) + S_i \quad (8)$$

$$D_i^{eff} = \varepsilon^{1.5} D_i \quad (9)$$

Equation (10) represents the energy conservation equation, where S_h is energy source term [12]:

$$\nabla \cdot (\rho C_p \vec{u} T) = -\nabla \cdot (k \nabla \mathrm{T}) + S_h \quad (10)$$

$$S_h = I^2 R_{ohm} + h_{react} - j_{an,ca}\, \eta_{an,ca} \quad (11)$$

The potential equations are presented in equations (12) and (13) [19].

$$\nabla . (\sigma_{sol} \nabla \varphi_{sol}) + S_{sol} = 0 \quad (12)$$

$$\nabla . (\sigma_{mem} \nabla \varphi_{mem}) + S_{mem} = 0 \quad (13)$$

The fuel and oxidant enter the flow channels at constant mass flow rates and temperatures, while a pressure boundary condition is specified at the channel outlets. A constant temperature condition is applied to the external walls. Furthermore, the electric potential is set to zero at the anode side and to the fuel cell voltage at the cathode side.

The model was implemented using the finite volume method through the fuel cell module in ANSYS Fluent. Furthermore, the discretization of the governing equations was carried out using the second-order upwind scheme, and the SIMPLE algorithm was employed to couple velocity and pressure.

4. Results and Discussion

The current density–voltage curve (polarization curve) for different flow configurations is presented in Figure 2. As observed, in all cases the current density initially decreases sharply with a reduction in voltage, then the rate of decrease slows down, and subsequently increases again. Figure 2 further illustrates that the current densities in Cases 4 and 5 (corresponding to counter-flow configurations) are higher than those of the other cases. In the counter-flow arrangement, the outlet of one cell aligns with the inlet of the adjacent cell, creating a stronger concentration gradient between the two neighboring cells. This enhanced gradient facilitates the diffusion of reactant species into the active regions, thereby intensifying the electrochemical reactions and resulting in higher current density.

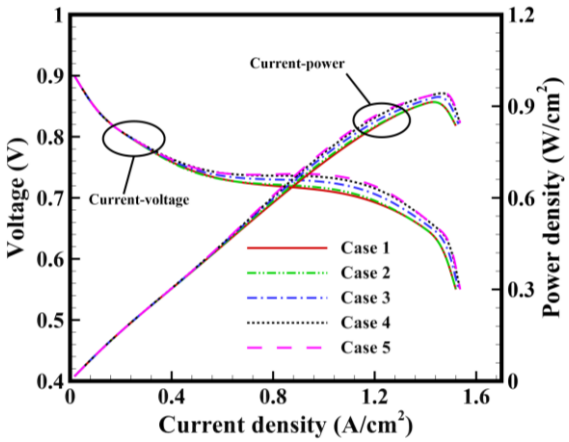

Figure 2. Current density–voltage curves at an air stoichiometric ratio of 1.1

Figure 3 illustrates the current density–voltage curve at an air stoichiometric ratio of 2.2. Figure 3 shows that increasing the air stoichiometric ratio reduces the voltage drop at high current densities, as a greater amount of oxygen becomes available at the cathode electrode.

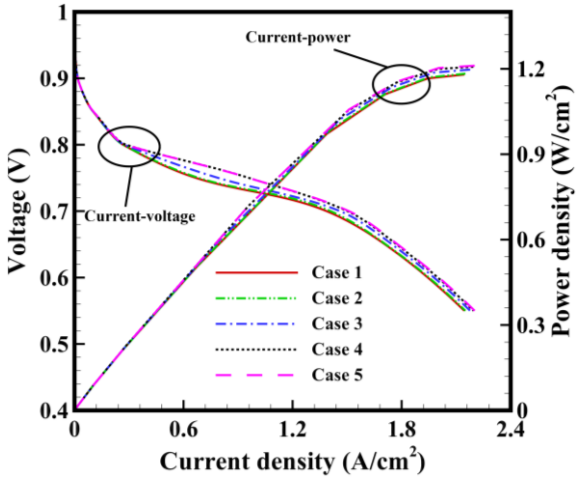

Figure 3. Current density–voltage curves at an air stoichiometric ratio of 2.2

Figure 4 compares the maximum temperature gradients for different cases in three directions: width (X), height (Y), and length (Z). The results indicate that, in all cases, the temperature gradient is largest in the vertical direction and smallest in the longitudinal direction. This difference is attributed to the physical geometry of the fuel cell. Since the height of the fuel cell is relatively small, even minor temperature variations in this direction lead to a comparatively large gradient. In contrast, the cell length is considerable, and the gas flow moves along this direction, continuously transporting heat. Therefore, although the overall temperature difference along the channel may be significant, the temperature gradient in the longitudinal direction remains smaller compared to the other directions due to the extended path length.

Furthermore, cases 1 and 2, in which both cells operate under co-flow configuration, exhibit lower temperature gradients. In contrast, the counter-flow configurations (cases 4 and 5) experience larger temperature gradients. Based on the results, the minimum maximum temperature gradient is 3.84 K/cm, observed in case 1, while the maximum value of 7.88 K/cm occurs in case 4.

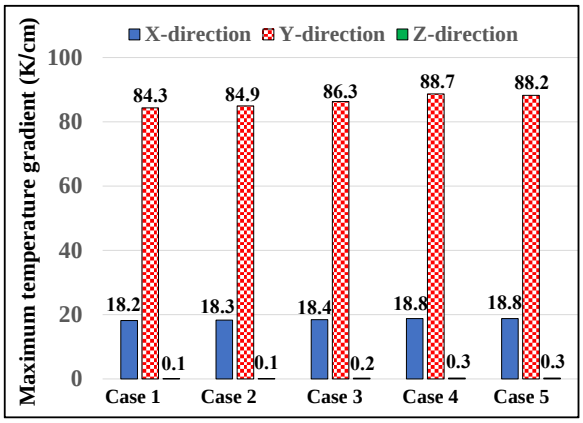

Figure 4. Comparison of maximum temperature gradients along the three directions

5. Conclusion

The present study has numerically investigated the effect of different inlet gas flow directions on the thermal and electrochemical performance of two adjacent PEMFC cells. The governing equations have been solved under steady-state, three-dimensional conditions using the finite volume method in ANSYS Fluent. The main findings of this study can be summarized as follows:

- Counter-flow configurations within PEMFC enhance electrochemical performance, as observed in Cases 4 and 5. In contrast, Cases 1 and 2, where both cells operate in co-flow mode, exhibit similar performance and the lowest output current densities.
- The convergence of output current densities at

low voltages is attributed to limited reactant availability at the cathode. increasing the cathode mass flow rate improves reactant transport to the catalyst layer, thereby increasing the output current density.

- Temperature gradient along the vertical direction is the highest, whereas the temperature gradient along the longitudinal direction is the lowest.
- Cases 1 and 2, in which both cells follow co-flow pattern, experience smaller temperature gradients. Conversely, cases with counter-flow in both cells (Cases 4 and 5) exhibit larger thermal gradients.

6. References

[1] Yuan Y, Abdullah M, Sajadi SM, Heidarshenas B, Malekshah EH, Aybar HŞ (2024) Numerical investigation of the effect of changing the geometry of a U-shaped fuel cell channel with asymmetric gas flow and its effect on hydrogen consumption. *Int J Hydrogen Energy* 50: 1167-1178.

[2] Alaedini AH, Tourani HK, Saidi M (2023) A review of waste-to-hydrogen conversion technologies for solid oxide fuel cell (SOFC) applications: Aspect of gasification process and catalyst development. *J Environ Manage* 329: 117077.

[3] Ganjian M, Alirezapouri MA, Farahabadi HB (2024) Fuel Cell-Based Hybrid Ship Design. *J Solid Fluid Mech* 14(2): 15-29.

[4] Yang X, Meng X, Sun J, Song W, Sun S, Shao Z (2023) Study on internal dynamic response during cold start of proton exchange membrane fuel cell with parallel and serpentine flow fields. *J Power Sources* 561: 232609.

[5] Qiao JN, Guo H, Ye F, Chen H (2024) A nonlinear contraction channel design inspired by typical mathematical curves: Boosting net power and water discharge of PEM fuel cells. *Appl Energy* 357:122474.

[6] Meng H, Song J, Guan P, Wang H, Zhao W, Zou Y, Ding H, Wu X, He P, Liu F, Zhang Y (2024) High ion exchange capacity perfluorosulfonic acid resine proton exchange membrane for high temperature applications in polymer electrolyte fuel cells. *J Power Sources* 602: 234205.

[7] Lim K, Vaz N, Lee J, Ju H (2020) Advantages and disadvantages of various cathode flow field designs for a polymer electrolyte membrane fuel cell. *Int J Heat Mass Transf* 163: 120497.

[8] Qiu D, Peng L, Lai X, Ni M, Lehnert W (2019) Mechanical failure and mitigation strategies for the membrane in a proton exchange membrane fuel cell. *Renew Sustain Energy Rev* 113: 109289.

[9] Hami M, Mahmoudimehr J (2025) Influence of flow configuration on heat-up and start-up processes of multi-channel solid oxide fuel cell: A comprehensive multi-criteria study. *Appl Therm Eng* 264: 125526.

[10] Bilgili M, Bosomoiu M, Tsotridis G (2015) Gas flow field with obstacles for PEM fuel cells at different operating conditions. *Int J Hydrogen Energy* 40(5): 2303-2311.

[11] Rezazadeh S, Rasouli Garaveran M, Ahmadi N, Sadeghi H (2020) Experimemtal and Numerical Analysis of Bipolar width and Gas Channels Geometrical Configuration Effect on Proton Exchange Membrane Fuel cell. *J Solid Fluid Mech* 10(4): 357-372.

[12] Pashaki MK, Mahmoudimehr J (2023) Performance superiority of an arc-shaped polymer electrolyte membrane fuel cell over a straight one. *Int J Hydrogen Energy* 48(36): 13633-13649.

[13] Fu L, Lin H, Liu J, Hua Z, Qiu N (2024) Optimization of sinusoidal wave-like channel design for HT-PEMFCs based on genetic algorithm. *Int J Heat Mass Transf* 232: 125964.

[14] Yang X, Xiang Q, Fang D, Sun S, Hao J, Xie F, Shao Z (2024) Simulation and experimental investigation of a novel chain-shaped flow field for proton exchange membrane fuel cell. *Energy Convers Manag* 315:118797.

[15] Li H, Xu B, Lu G, Du C, Huang N (2021) Multi-objective optimization of PEM fuel cell by coupled significant variables recognition, surrogate models and a multi-objective genetic algorithm. *Energy Convers Manag* 236:114063.

[16] Akbari MH, Rismanchi B (2008) Numerical investigation of flow field configuration and contact resistance for PEM fuel cell performance. *Renew Energy* 33(8):1775-1783.

[17] Siegel NP, Ellis MW, Nelson DJ, von Spakovsky MR (2004) A two-dimensional computational model of a PEMFC with liquid water transport. *J Power Sources* 128: 173-184.

[18] Guvelioglu GH, Stenger HG (2005) Computational fluid dynamics modeling of polymer electrolyte membrane fuel cells. *J Power Sources* 147(1-2):95-106.

[19] Toghyani S, Nafchi FM, Afshari E, Hasanpour K, Baniasadi E, Atyabi S (2018) Thermal and electrochemical performance analysis of a proton exchange membrane fuel cell under assembly pressure on gas diffusion layer. *Int J Hydrogen Energy* 43(9): 4534-4545.